

## Production of Mesons by X-Rays

Edwin M. McMillan, Jack M. Peterson, and R. Stephen White<sup>1</sup>

*Radiation Laboratory, Department of Physics,  
University of California, Berkeley*

AT THE 1949 SPRING MEETING of the National Academy of Sciences (2) a preliminary account was given of some observations of mesons produced by the 335-Mev x-ray beam from the Berkeley synchrotron. The present paper is a progress report of this work; no claim is made for completeness, but sufficient new data are available to make publication at this time worth while, especially since some of the numerical results given in the earlier report require revision.

The x-ray beam, produced by the impact of 335-Mev electrons on a 20-mil-thick platinum target, has a width at half-maximum of 0.0135 radian (about 1 inch at 6 feet from the target). In all but the earliest experiments the beam was further defined by a 1-inch hole in a lead block, then passed through a piece of carbon, which served as the meson source. The x-ray intensity at one meter from the target was about 3500 roentgens (r) per hour, measured behind  $\frac{1}{4}$ th inch of lead under the best running conditions; the average was about half this. The actual exposures at the carbon meson source (6 feet from the target) ranged from 500 to 2000 r in the later runs. Mesons were recorded on Ilford nuclear plates; the highest density of meson endings observed was about 100 per square centimeter in a 100-micron emulsion. In the following sections the experimental conditions and some of the results are described in more detail.

*Plate Exposure.* Plates have been exposed in the following ways:

**Geometry 1:** A stack of plates is traversed directly by the x-ray beam. Mesons are produced chiefly in the glass plates, and exposures are limited by the general blackening due to the beam. Meson tracks are counted in the part of the plates not overexposed by the central core of the beam. There is an appreciable background of photonuclear stars and proton tracks. Only Ilford F-3 plates were used in these exposures.

**Geometry 2:** The x-ray beam passes through a carbon slab, and the stacks of plates are placed alongside, out of the core of the beam. The intent was to deter-

mine the element in which the mesons are produced, but it was found that the wings of the beam had sufficient intensity at the location of the plates to make this somewhat doubtful, considering the fact that there was much more matter in the plates than in the carbon slab used. The background was considerably less than in Geometry 1, and longer exposures could be made; only F-3 plates were used.

**Geometry 3:** Same as Geometry 2, except that a lead collimator 6 in. thick with a 1-in. hole cuts off the wings of the beam. The x-ray intensity at the plates is now small, and they show little general blackening except along their leading edges; the heavy-particle background is very small. Both F-3 and C-2 plates were used.

**Geometry 4:** A modification of Geometry 3, with the following changes: A secondary collimator protects the plates from electrons scattered off the edge of the main collimator; the carbon slab is replaced by a cylinder of 1-in. diameter; stacks of plates are arranged radially around this cylinder, with different thicknesses of lead absorbers between the carbon and the plates, as shown in Figs. 1 and 2. Data reported for this geometry were all recorded on C-2 plates.

*Types of Meson Tracks.* The following types of features are seen at the ends of meson tracks in nuclear emulsions:

- (a) Stars of two or more prongs;
- (b) Stars of one prong;
- (c)  $\mu$ -meson tracks;
- (d) Small "blobs" of a few grains;
- (e) Nothing.

Events of type (a) and (e) are obviously recognizable, and require no further discussion. Events of type (d) are not always clearly enough defined to distinguish from (e), and therefore counts of these events cannot be used for statistical purposes, even though they probably represent vestigial stars, being due to the recoils following neutron ejection. In practice, (d) and (e) are lumped together as  $\rho$ -mesons.

Particular care is needed in distinguishing events of types (b) and (c) from one another. If the secondary track is heavy, it is clearly a star; if it is light, and of sufficient length to show the characteristic scattering and change in grain density, it is clearly a  $\mu$ -track. If it is light but leaves the emulsion too

<sup>1</sup>The authors thank the synchrotron crew for their help in making the exposures and W. S. Gilbert, E. Goodwin, W. J. Knox, G. Maenchen, and F. M. Smith for their assistance in scanning the plates. This work was supported by the Atomic Energy Commission.

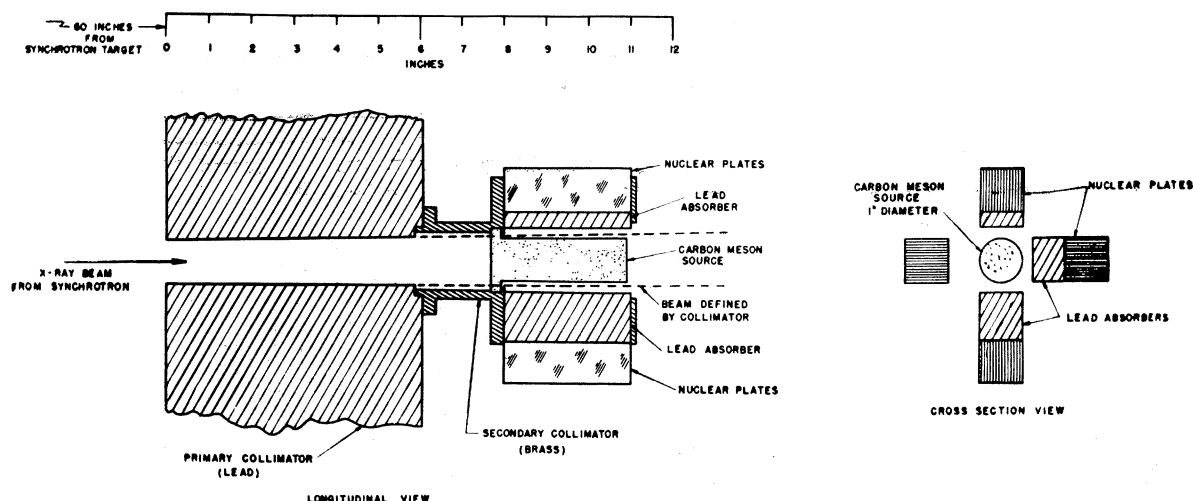


FIG. 1. Drawing of experimental arrangement (Geometry 4).

soon, there is a possibility of confusion. However, examination of magnetically sorted negative mesons produced in the cyclotron and recorded on Ilford C-2 plates shows that light single-pronged star tracks are almost invariably accompanied by blobs resulting from the recoil consequent on the emission of a very fast proton. Therefore, single light secondary tracks

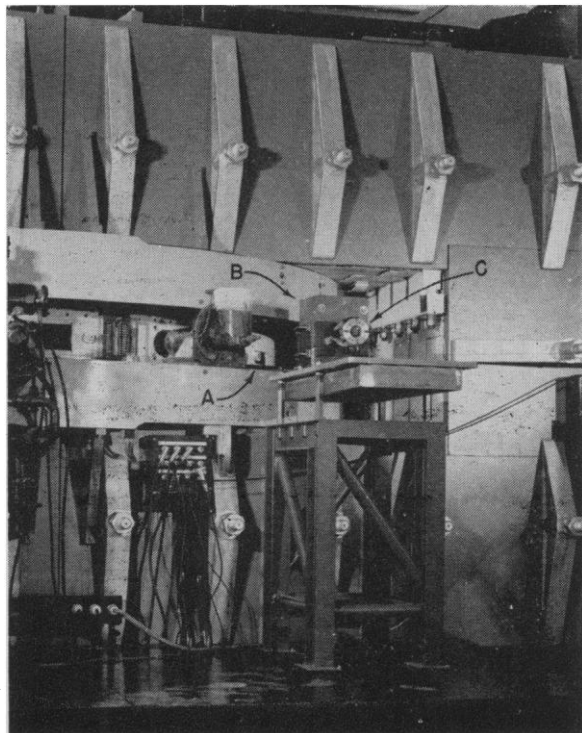


FIG. 2. Photograph of experimental arrangement (Geometry 4). The x-ray beam emerges from the synchrotron through the rectangular hole (A). The 6-inch-thick lead collimator is at B. C is the plate holder.

with no blobs are recorded as  $\mu$ -tracks, even though the observed range may not be long enough for positive identification.

We finally arrive at three classifications of meson track endings:

(a) + (b), denoted by  $\sigma$

(c), denoted by  $\pi\mu$

(d) + (e), denoted by  $\rho$ .

It is desired to compute from these the numbers of negative and positive  $\pi$ -mesons ( $\pi^-$  and  $\pi^+$ ) stopping in the emulsion.

*Methods of Computation.* (a) Computation of  $\pi^-$ . Negative  $\pi$ -mesons are assumed to be captured in the emulsion, and may or may not make recognizable stars. Therefore, it is important to know the fraction of cases in which stars are produced. Data on this are available from counts of tracks in Ilford C-2 plates due to magnetically sorted negative mesons (1). In these plates, it was found that the ratio  $\rho/(\sigma + \rho) = 0.27$ ; we deduce that, in Ilford C-2 plates,  $\pi^- = 1.37 \sigma$ . (b) Computation of  $\pi^+$ . *Method A.* If the plates are sufficiently sensitive to show the early parts of  $\mu$ -tracks with certainty, then the number  $\pi\mu$  is essentially equal to  $\pi^+$ . Experiments with magnetically sorted positive mesons (3) show that in C-2 plates at least 95 percent give recognizable  $\pi$ - $\mu$  decay. Therefore, when using these plates, it is assumed that  $\pi^+ = \pi\mu$ . The number  $\rho$  does not enter into this computation. *Method B.* If, on the other hand, less sensitive plates are used, as for example Ilford F-3, it is harder to recognize the  $\mu$ -tracks and a considerable fraction of them may be missed. Then a different method must be used, which is based on the assumption that all tracks not associated with negative  $\pi$  mesons, i.e., a number equal to  $\sigma + \pi\mu + \rho = 1.37 \sigma$ ,

consist of  $\pi^+$  tracks plus an equal number of  $\mu$  tracks. The distinction between  $\pi\mu$  and  $\rho$  does not enter into this calculation. This method may underestimate the true number, since the  $\mu$ -particles are emitted in random directions in the emulsion and glass of the plates, and therefore a certain fraction of these will end while crossing the emulsion at unfavorable angles for identification, while the  $\pi$ -particles are traveling approximately parallel to the emulsion. Without attempting to correct for this, the Method B calculation assumes that:

$$\pi^+ = \left(\frac{1}{2}\right) (\sigma + \pi\mu + \rho - 1.37\sigma).$$

**Results.  $\pi^-/\pi^+$  ratio.** At the time of writing the abstract for the National Academy meeting (2) 145 tracks were available, of which 51 were from Geometry 1 and 94 from Geometry 2. All of these were on F-3 plates, and therefore only Method B could be used for the computation, giving the published ratio  $\pi^-/\pi^+ = 10$ . By the time of the meeting, more tracks were available, including some on Geometry 3. The Geometry 1 tracks were then discarded, since they represent mesons starting in glass rather than carbon. The new total of 198 tracks (103 on Geometry 2 and 95 on Geometry 3), mostly on F-3 plates and analyzed by Method B, gave  $\pi^-/\pi^+ = 7.5$ , which was the value reported verbally at the meeting.

Since then, more tracks have become available, and it is now possible to give data obtained entirely with Geometry 4, using C-2 plates, and analyzed by Method A. Blank runs, with no carbon target in place, prove that virtually all the mesons seen actually originate in the carbon. In this setup there are plates behind lead absorbers, on which mesons of higher energy are recorded. The energy ranges are assumed to be defined by the stopping power of the absorber (including the radius of the carbon cylinder) for one limit, and that of the absorber plus the plate width for the other. No obliquity correction was applied. The values found for the ratio  $\pi^-/\pi^+$  in the various energy bands, covering a range from about 30 to 150 Mev, agree within the statistical errors, which are about  $\pm 25$  percent for bands about 10 Mev wide below 100 Mev, and  $\pm 50$  percent for a band between 100 and 150 Mev. Since there is no statistically significant evidence for a variation with meson energy, the data are lumped together, including only track counts made or checked by experienced observers. These counts are:  $\sigma = 403$ ,  $\pi\mu = 327$ ,  $\rho = 323$ . Using Method A, the ratio  $\pi^-/\pi^+ = 1.7$ , with a statistical standard error of 8 percent. Method B applied to the same data gives  $\pi^-/\pi^+ = 2.2$ , indicating the sort of error to be expected when the latter is used with C-2 plates; it may be still greater with F-3 plates, on which the tracks are harder to find. It will be noted that this ratio is less than the previously given values. The

difference from the earlier values may be partly real, that is, the Coulomb effect for very low energy mesons made in glass may distort the ratio somewhat; a considerable part of the difference certainly comes from the errors inherent in the use of Method B with

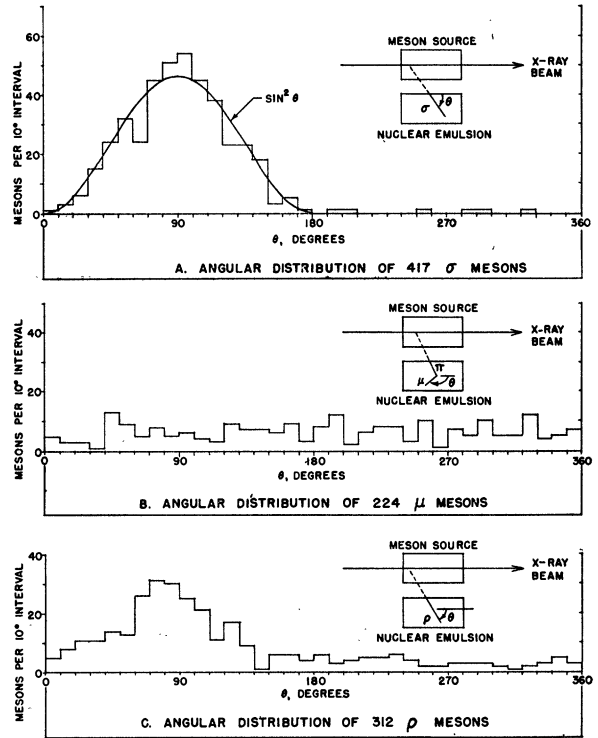


FIG. 3. Angular distributions of meson tracks in the energy range 43 to 59 Mev. (A)  $\sigma$ -Mesons. The curve  $\sin^2 \theta$  represents approximately the distribution to be expected in case of spherically symmetrical emission from all parts of the carbon target. The few tracks in the range  $180^\circ$  to  $360^\circ$  were probably scattered.  $\pi$ -Mesons associated with  $\pi\mu$ -decay give a similar distribution. (B)  $\mu$ -Mesons associated with  $\pi\mu$ -decay. There is no evidence here of departure from spherical symmetry. (C)  $\rho$ -Mesons. This distribution is clearly composite, the peak at  $90^\circ$  being due to  $\pi^-$  mesons that fail to make visible stars, while the uniform background is due to  $\mu$ -mesons.

F-3 plates, and some may be attributed to inexperience of the observers in the beginning.

The ratio of 1.7 does not pose the formidable theoretical problem offered by the earlier value; in fact a ratio of this order can be explained on rather elementary grounds. Consider the products of the reactions, which are  $\pi^-$  and  $\pi^+$  in one case, and  $\pi^+$  and  $n^0$  in the other. The current accompanying the process is greater in the former because of the contribution of the recoil proton, and therefore the coupling to the photon field is larger. This effect, which increases with meson energy, plus the Coulomb effect on the meson wave function, which decreases with energy, together can account for the observed ratio. A de-

tailed discussion of this will be given in a later publication by K. A. Brueckner.

*Yield of Mesons. Energy and Angle Distributions.* From the data obtained with Geometry 4, some information can be gained on the distribution of mesons in angle and energy, as well as the total yield. The distribution of angles of the straight parts of the tracks (excluding of course  $\mu$  and  $\rho$  tracks) is consistent with that to be expected for an isotropic emission from all parts of the carbon target. The computed distribution on this assumption, in the case of the plates covering the band 43 to 59 Mev, can be represented approximately by  $\sin^2 \theta$ . Fig. 3A shows that the data agree with this. Higher energy plates show the expected narrower distribution, and lower energy plates a slightly wider one. The conclusion is that the initial meson distribution has at least roughly spherical symmetry. In order to compute the total number of mesons in a given energy range, we then use the fact that an ideal infinite line source would give a uniform angular distribution, whose height would be equal to the observed height at  $90^\circ$ . The height is computed by fitting the expected shape to the observed distribution—or, what is the same thing, the total number is taken to be the observed number multiplied by a "shape factor," which is just 2 in the case of the  $\sin^2 \theta$  distribution.

The differential yield  $\frac{dN}{dE}$  can now be computed from the following formula:

$$\frac{dN}{dE} = 4r \frac{dR}{dE} \frac{1.37 \sigma + \pi\mu}{At} \times \text{shape factor},$$

where  $N$  = No. of mesons produced per cm length of target

$E$  = energy of mesons

$r$  = radius to center of area scanned

$R$  = range of mesons in glass or emulsion (these are nearly equal)

$\sigma$ ,  $\pi\mu$  are track counts in area  $A$  of emulsion

$t$  = thickness of emulsion during exposure (a shrinkage factor of 2.4 was used).

The shape factor varies from 1.8 to 4.3.

The results, normalized to an exposure of 1 r, are given in Fig. 4, with standard errors from the track counting statistics alone. The most likely other errors are losses at the low energy end from self-absorption in the carbon, and at the high energy end from scattering in the lead absorbers.

The absolute value of the cross section can be obtained from the integral of Fig. 4, if the number of quanta corresponding to the rather arbitrary unit "r behind  $\frac{1}{8}$ th inch of Pb" is known. This has been measured, using a thin air chamber intercepting the whole beam as defined by the collimator, with thin layers of

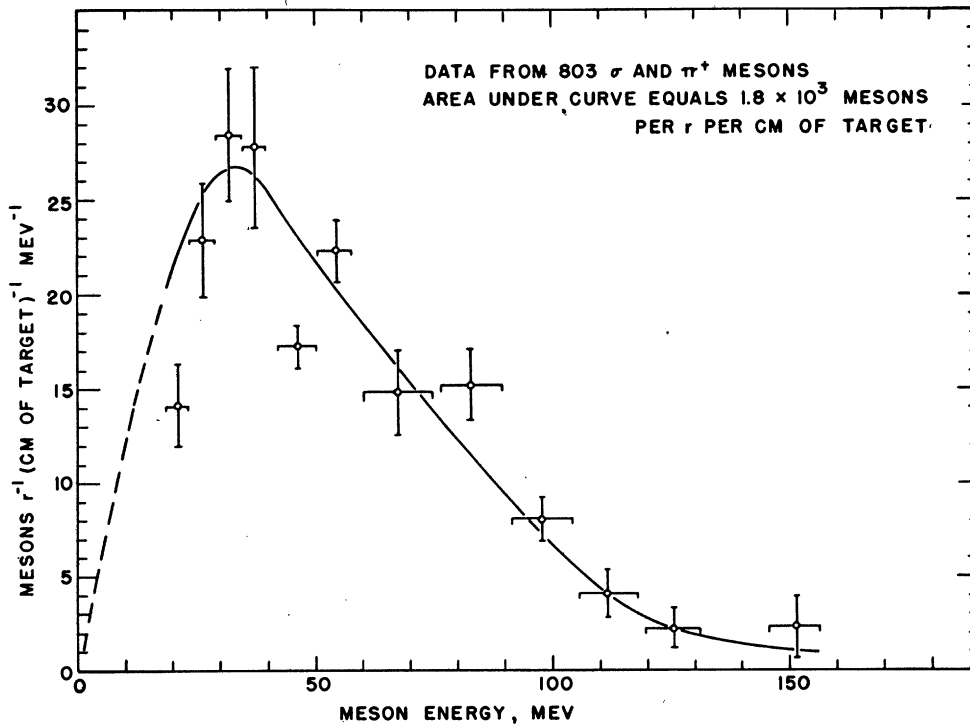


FIG. 4. Distribution of meson energies from x-ray energy of 335 Mev. The apparent lower limit on the energy is caused by the fact that the energies are computed as if the mesons originated in the center of the carbon block. The dotted line is simply a guess as to the trend of the distribution at low energies, which was used in the integration leading to the total cross section.

lead and other substances in front in order to be able to estimate the amount of the ionization due to pair production alone. This will be described in detail in a later publication; the result was that 1 r on the carbon corresponds to  $4.9 \times 10^7$  quanta traversing it, where the number of quanta is defined as the total x-ray energy divided by the upper limit energy. (The actual number of quanta in a range between  $E_1$  and  $E_2$  is approximately  $\ln (E_2/E_1)$  times the above number.) The total cross section per quantum per carbon nucleus is then found to be  $5 \times 10^{-28}$  cm<sup>2</sup>. It is hard to make an estimate of the over-all accuracy of this figure, but it is probably not wrong by more than a factor of 2. The difference between this value and that given in reference 2 is easy to under-

stand, since the latter, made from Geometry 1 plates, included only very low energy mesons. One run was made at an x-ray energy of 200 Mev; here the meson energy distribution extends only to about 35 Mev, and the yield is considerably less than at 335 Mev. Because of the large self-absorption of the mesons at this energy, no attempt was made to calculate a cross section.

#### References

1. ADELMAN, F. L. and JONES, S. B. *Phys. Rev.*, 1949, **75**, 1468.
2. McMILLAN, E. M. and PETERSON, J. M. *Science*, 1949, **109**, 438.
3. SMITH, F. M. Private communication.

## Experimental Control in Hypnotic Age Regression States

Robert M. True

*University of Vermont College of Medicine, Burlington*

THE RECOVERY OF EARLY CHILDHOOD MEMORIES, lost through the ordinary processes of forgetting or because of subconscious repression, has a definite place in modern psychotherapy. The importance of catharsis has long been recognized, but too little work has been carried out to determine whether hypnotic age regression is a fact, or, as Young (4) believes, an artifact. Too few adequately controlled experiments have been carried out which separate and distinguish between half-conscious dramatization of current memories of a previous time and actual revivification of behavior patterns of a suggested earlier period of life in terms of what actually belongs there. Since both conditions may exist during a sitting, the importance of constant control cannot be overemphasized. Erickson and Kubie (1) recognized the existence of these two states and yet utilized hypnotic age regression with a great deal of success in the treatment of hysteria without determining which state was involved. The fact that psychotherapy based upon a supposed memory is of value to a patient is hardly satisfactory evidence of a true regression, since it is always possible that a pseudomemory may be effective in such a case (3). This has been shown quite con-

clusively in the use of play or dramatic therapy, both in the waking state and during hypnosis.

Information from relatives, verbal material memorized at an early age, and diaries are unsatisfactory controls, since the normal processes of forgetting must be considered in the first case, the possibility of review in the second, and the recognized inaccuracy of diaries written at an early age in the last case. The factor of the recall of very recently learned material may be of value from an academic viewpoint but is obviously unsatisfactory for hypnoanalytical purposes, where remote memories are of primary importance.

For the most part, the use of hypnosis in age regression has been interpreted in terms of a hypothetical state called *dissociation*. Psychoanalysis and hypnoanalysis are actually doctor-patient battles, with the patient trying to retain his compulsions and the operator equally determined to eliminate them. The evidence points at the fact that the recall of actual traumatic experience is more efficacious in bringing about beneficial results in the treatment of a neurosis than the reliving of an imagined experience (2), although it must be recognized that neither one invariably brings about the desired therapeutic change.